THE JOURNAL OF BIOLOGICAL CHEMISTRY VOL. 284, NO. 33, pp. 22444–22456, August 14, 2009
© 2009 by The American Society for Biochemistry and Molecular Biology, Inc. Printed in the U.S.A.

The PRY/SPRY/B30.2 Domain of Butyrophilin 1A1 (BTN1A1) Binds to Xanthine Oxidoreductase

IMPLICATIONS FOR THE FUNCTION OF BTN1A1 IN THE MAMMARY GLAND AND OTHER TISSUES[*][S]

Received for publication, May 12, 2009 Published, JBC Papers in Press, June 15, 2009, DOI 10.1074/jbc.M109.020446

Jaekwang Jeong[‡1], **Anita U. Rao**[‡1], **Jinling Xu**[‡], **Sherry L. Ogg**[‡], **Yetrib Hathout**[§], **Catherine Fenselau**[§], **and Ian H. Mather**[‡2]

From the Departments of [‡]*Animal and Avian Sciences and* [§]*Chemistry and Biochemistry, University of Maryland, College Park, Maryland 20742*

Butyrophilin 1A1 (BTN1A1) and xanthine oxidoreductase (XOR) are highly expressed in the lactating mammary gland and are secreted into milk associated with the milk fat globule membrane (MFGM). Ablation of the genes encoding either protein causes severe defects in the secretion of milk lipid droplets, suggesting that the two proteins may function in the same pathway. Therefore, we determined whether BTN1A1 and XOR directly interact using protein binding assays, surface plasmon resonance analysis, and gel filtration. Bovine XOR bound with high affinity in a pH- and salt-sensitive manner (K_D = 101 ± 31 nM in 10 mM HEPES, 150 mM NaCl, pH 7.4) to the PRY/SPRY/B30.2 domain in the cytoplasmic region of bovine BTN1A1. Binding was stoichiometric, with one XOR dimer binding to either two BTN1A1 monomers or one dimer. XOR bound to BTN1A1 orthologs from mice, humans, or cows but not to the cytoplasmic domains of the closely related human paralogs, BTN2A1 or BTN3A1, or to the B30.2 domain of human RoRet (TRIM 38), a protein in the TRIM family. Analysis of the protein composition of the MFGM of wild type and BTN1A1 null mice showed that most of the XOR in mice lacking BTN1A1 was released from the MFGM in a soluble form when the milk lipid droplets were disrupted to prepare membrane, compared with wild-type mice, in which most of the XOR remained membrane-bound. Thus BTN1A1 functions *in vivo* to stabilize the association of XOR with the MFGM by direct interactions through the PRY/SPRY/B30.2 domain. The potential significance of BTN1A1/XOR interactions in the mammary gland and other tissues is discussed.

Members of the butyrophilin (BTN)[3] gene family are attracting increasing attention because they may play multifunctional roles in diverse physiologies, including lactation (1, 2), selection and regulation of T-cells in the immune system (3–6), and modulation of autoimmune disease (7–9). BTN proteins have the canonical structures of cell surface receptors, which, after an N-terminal signal sequence, generally comprise two exoplasmic Ig folds (10, 11), a membrane anchor and a cytoplasmic domain consisting of a stem region, a PRY/SPRY/B30.2 domain (12, 13), and a cytoplasmic tail at the C terminus (14).

The eponymous BTN1A1 protein has been linked to the secretion of milk lipid droplets because it is highly expressed in the mammary epithelium during lactation and is incorporated into the surface membrane coat surrounding cytoplasmic lipid droplets (the milk fat globule membrane (MFGM)) as they bud into milk from the apical surface (15). Furthermore, ablation of the *Btn1a1* gene disrupts lipid secretion, causing the accumulation of large pools of triacylglycerol in the cytoplasm of *Btn1a1* null mice (1). In a different context, dietary exposure to BTN1A1 in dairy products has been associated with modulation of the autoimmune disease multiple sclerosis because of structural similarities between the IgI fold of BTN1A1 (16) and the IgV fold of myelin oligodendrocyte glycoprotein (MOG) (17) an antigen on the myelin nerve sheath that is a target for autoantibodies in multiple sclerosis patients (8–10).

Potential interactions between the exoplasmic Ig folds of several BTN proteins, and putative receptors on immune cells are postulated to regulate positive selection of epidermal γδ-T cells in the case of Skint1 (6) and suppress T-cell activation in the case of BTNL2 (4, 5). In addition, BTN2A1 binds to the C-type lectin, DC-SIGN, on immature dendritic cells (18), and proteins in the BTN3A1–3 subfamily bind to an unidentified ligand on various immune cells (19).

Interactions between the cytoplasmic domain of BTN and intracellular proteins have not been investigated in any detail. The intracellular region of most BTNs is dominated by the

* This work was supported, in whole or in part, by National Institutes of Health Grant R01 HD048588-01A1. This work was also supported by United States Department of Agriculture Grants NRI 0003264 and 2005–04637 and the Maryland Agricultural Experiment Station (to I. H. M.).

[S] The on-line version of this article (available at http://www.jbc.org) contains supplemental Tables 1S and 2S and Figs. 1S–3S.

[1] Both of these authors contributed equally to this work.

[2] To whom correspondence should be addressed: Dept. of Animal and Avian Sciences, University of Maryland, College Park, MD 20742. Tel.: 301-405-1380; Fax: 301-405-7980; E-mail: imather@umd.edu.

[3] The abbreviations used are: BTN, butyrophilin (orthologs of BTN in mice, cows, and humans are denoted mBTN, bBTN, and hBTN, respectively, and paralogs are denoted by the appropriate designation (*e.g.* hBTN1A1, hBTN2A1, and hBTN3A1); BTN1A1cyto, cytoplasmic domain of BTN1A1; GST, glutathione *S*-transferase; ECFP, enhanced cyan fluorescent protein; EYFP, enhanced yellow fluorescent protein; GFP, green fluorescent protein; bXOR and bB30.2, bovine XOR and B30.2, respectively; mXOR and mB30.2, mouse XOR and B30.2, respectively; MFGM, milk fat globule membrane; PBS, phosphate-buffered saline; SPR, surface plasmon resonance; TBS, Tris-buffered saline; XOR, xanthine oxidoreductase; MOG, myelin oligodendrocyte glycoprotein; RIPA, radioimmune precipitation; FPLC, fast protein liquid chromatography; MES, 4-morpholineethanesulfonic acid; Tricine, *N*-[2-hydroxy-1,1-bis(hydroxymethyl)ethyl]glycine.

B30.2 or the PRY/SPRY domain, which comprises two sheets of antiparallel β-strands folded into a β- sandwich, which in some proteins is contiguous at the N terminus with one or two α-helices (20–24) (for a discussion of the relationship between PRY, SPRY, and B30.2 domains, see Ref. (25)). This domain (here abbreviated as B30.2),[4] is postulated to serve as a protein-binding module, by which proteins interact through the extended surface loops that adjoin individual β-strands (22).

One protein that may bind to the cytoplasmic region of BTN proteins (and the B30.2 domain) is the redox enzyme, xanthine oxidoreductase (XOR),[5] because it was shown to bind to the cytoplasmic domain of mouse BTN1A1 in an *in vitro* binding assay (26). Furthermore, one XOR-deficient mouse strain ($Xdh^{+/-}$) (27) displayed a lactation phenotype similar to that of *Btn1a1* null mice (1), suggesting that the two proteins may be functionally linked by direct interaction. These conclusions, however, have been challenged, because XOR does not co-localize with BTN1A1 in immunolabeled freeze-fractured replicates of secreted milk lipid droplets (28), and a second mouse strain deficient in XOR does not appear to have an altered lactation phenotype (29).

In this paper, we devise *in vivo* and *in vitro* assays to show that the cytoplasmic domain of BTN1A1 binds to XOR via the B30.2 domain and that BTN1A1 is required for the stable association of XOR with the MFGM *in vivo*. Furthermore, interaction with XOR appears to be limited to BTN1A1 orthologs. These results are discussed in the context of potential functions of BTN1A1 in the mammary gland and other tissues and the relationship of BTN1A1 to other BTN family members.

EXPERIMENTAL PROCEDURES

Materials—Reduced glutathione, vitamins, amino acids, pepstatin A, leupeptin, N^{α}-*p*-tosyl-L-lysine chloromethyl ketone, N^{α}-*p*-tosyl-L-phenylalanine chloromethyl ketone, aprotinin, digitonin, and adjuvants were obtained from Sigma. The ESP® yeast protein expression and purification system was from Stratagene (La Jolla, CA). Glutathione-coated beads for the purification of glutathione *S*-transferase (GST) fusion proteins, thrombin, ECL Western blot detection reagents, supplies for surface plasmon resonance (SPR), cyanogen bromide-activated Sepharose 4B, and protein A-coated Sepharose beads were from Amersham Biosciences/GE Healthcare. Rabbits were purchased from Covance (Princeton, NJ). Horseradish peroxidase-conjugated goat anti-rabbit secondary antibody (blotting grade), Triton X-100, SDS, acrylamide, and bisacrylamide were from Bio-Rad, and protease inhibitor tablets were from Roche Applied Science. DNA polymerases, restriction enzymes, dNTPs, and trypsin were from Promega (Madison, WI), and phenylmethylsulfonyl fluoride and keyhole limpet hemocyanin were obtained from Calbiochem. Lipofectamine, rabbit anti-green fluorescent protein (GFP) antibody, and Dulbecco's phosphate-buffered saline (PBS) were from Invitrogen. All other chemicals were from Fisher.

Expression and Purification of Recombinant Proteins—Recombinant proteins were expressed in *Schizosaccharomyces pombe*, because the genome does not contain the XOR gene (30). Potential interactions between BTN and endogenous XOR were thus avoided. cDNAs were inserted 3′ to the GST gene in the pESP-1 vector supplied with the ESP-Yeast Protein Expression and Purification System (Stratagene) (see supplemental Table 1S for details, definitions, nomenclature, and abbreviations for the vectors used). Deletion constructs were prepared using PCR (see supplemental Table 2S for primer pairs). SP-Q01 *S. pombe* cells were transformed with the completed vectors and grown in 1l cultures, as recommended by the manufacturer. In initial experiments, cells were resuspended in a mixture of 140 mM NaCl, 2.7 mM KCl, 10 mM Na_2HPO_4, and 1.8 mM KH_2PO_4 (PBS1) and lysed by vortexing with glass beads for 5–7 min in the presence of proteinase inhibitors (1 mM phenylmethylsulfonyl fluoride, 1 μl/ml aprotinin (8.2 IU/ml), 1 μM pepstatin A, 100 μM leupeptin) and 0.5% (v/v) Triton X-100. In later experiments, improved yields of protein (6–10 mg of protein/liter) were obtained by resuspending the cells in a modified lysis buffer (150 mM NaCl, 0.5 mM EDTA, 50 mM Tris-HCl, pH 7.4, Roche Applied Science protease inhibitors, 1 mM phenylmethylsulfonyl fluoride, and 1 μl/ml aprotinin (8.2 IU/ml)) and breaking the cells with a French press. Lysates were clarified by centrifugation at 17,000 × g_{av} for 30 min, followed by 34,000 × g_{av} for 1 h in a Beckman model XL-90 ultracentrifuge. Recombinant proteins were purified by chromatography on glutathione resins following standard procedures.

Preparation of Thrombin-cleaved Proteins—GST was removed from the recombinant proteins by digestion with thrombin (GE Healthcare). ~5-mg batches of purified fusion protein were rebound to glutathione-Sepharose beads and incubated overnight with gentle agitation at 22 °C in 5.0 ml of 20 mM Tris-HCl buffer, pH 8.4, containing 150 mM NaCl, 2.5 mM $CaCl_2$, and thrombin (10 NIH enzyme units/mg of fusion protein). The recombinant protein was recovered from the supernatant, and the thrombin was removed by gel filtration on Superdex 200.

Preparation of Vectors Encoding Fluorescent Fusion Proteins of mBTN1A1 and mXOR—Total RNA was purified from lactating mouse mammary gland using TRIzol reagent (Invitrogen) and XOR and BTN1A1 cDNAs prepared by reverse transcription-PCR using the SuperScript™ III One-Step RT-PCR kit from Invitrogen and specific primers complementary to the 5′ and 3′ mouse *Xdh* and *Btn1a1* open reading frames, respec-

[4] The B30.2 domain was first defined as a region of similarity in linear sequence encoded by a single exon in BTN and TRIM protein genes (12). Recent structural determinations of PRY-SPRY-19q13.4.1, GUSTAVUS, TRIM21, and SOCS box protein 2 (SSB-2) (20, 21, 23, 24) have shown that this exon encodes the β-sandwich. However, in some cases, additional N-terminal α-helices, encoded by adjacent 5′ exons are an integral part of the entire domain and may play a role in the domain's stability. Secondary structure predictions using NPSA and Jpred programs suggest that the equivalent BTN1A1 domain will also contain N-terminal α- helices. Therefore, the term "B30.2" is used throughout this paper to include both the predicted N-terminal α-helices (outside of the historical B30.2 domain) and the β- sandwich (for hBTN1A1, residues 285–476; see Fig. 2 of Ref. 21 for sequence alignments and further details).

[5] The enzyme is expressed in most tissues as xanthine dehydrogenase. Conversion to the oxidase form occurs in the mammary gland during or following secretion into milk (see Ref. 1 for discussion). For convenience, the protein is denoted throughout as xanthine oxidoreductase (XOR), regardless of whether it is in the dehydrogenase or the oxidase form. According to international convention, the genes encoding human and bovine BTN1A1 and XOR are denoted *BTN1A1* and *XDH*, respectively, and the mouse genes are denoted *Btn1a1* and *Xdh*, respectively.

tively. The region of the cDNA encoding the processed form of mBTN1A1 with the N-terminal signal sequence removed was amplified with a second set of primers (supplemental Table 2S), which introduced XhoI and XmaI restriction enzyme sites into the 5′- and 3′-ends, respectively, and the amplified product was cloned into the pECFP-C1 vector (Clontech Living Color vectors), which had been mutated so as to encode monomerized ECFP (enhanced cyan fluorescent protein). The signal peptide of mBTN1A1 was then inserted 5′ of the ECFP gene using primers incorporating NheI and AgeI restriction enzyme sites at the 5′- and 3′-ends, respectively. The completed vector thus encoded the mBTN1A1 signal sequence, followed by the ECFP gene fused to the mature form of mBTN1A1. Deletion constructs (supplemental Table 1S) were prepared by amplifying the appropriate regions of the open reading frame of *Btn1a1* using the primers listed in supplemental Table 2S. A vector encoding mXOR with monomerized EYFP (enhanced yellow fluorescent protein) at the C terminus was constructed using primers encoding NheI and XmaI restriction enzyme sites at the 5′- and 3′- ends, respectively (supplemental Table 2S), and the amplified product cloned into the pEYFP-N1 vector (Clontech). All PCR products were verified by sequencing.

Affinity Chromatography of Tissue Extracts on a Glutathione Matrix—C3H mice were killed on day 10 of lactation by asphyxiation in CO_2, and all of the mammary glands were excised and weighed. Connective and adipose tissue were removed, and three volumes of Tris-buffered saline (TBS; 10 mM Tris-HCl, 140 mM NaCl, pH 7.2) containing proteinase inhibitors (0.1 mM phenylmethylsulfonyl fluoride, 0.1 mM N^{α}-*p*-tosyl-L-lysine chloromethyl ketone, 0.1 mM N^{α}-*p*-tosyl-L-phenylalanine chloromethyl ketone, 1.0 ml/100 ml (8.2 IU/ml) aprotinin, and 1 mM ϵ-aminocaproic acid) were added per g of tissue. The tissue was minced finely and homogenized on ice using a Polytron homogenizer by giving five pulses of 10 s each at a speed setting of eight. Homogenates were filtered through two layers of cheesecloth premoistened with TBS, and the filtrates were centrifuged at 1,000 × g_{av} for 10 min at 4 °C to obtain sediments, operationally called the nuclear pellet. The postnuclear supernatants were further centrifuged at 100,000 × g_{av} at 4 °C for 1 h, and the resulting postmicrosomal supernatants were retained for analysis. Postmicrosomal supernatants (50 mg of protein) were fractionated on 2-ml glutathione affinity columns, which had been saturated previously with either GST-mBTN1A1cyto (test column) or GST (control column). The columns were washed with PBS1, and bound protein was eluted with 10 ml of 10 mM reduced glutathione. Fractions containing protein were combined and analyzed by SDS-PAGE. The entire procedure was repeated a total of three times with similar results.

Cell Expression Assay for Protein Binding—HEK 293T cells were grown to 80–90% confluence in 20 × 10 × 10-mm LAB-Tek culture chambers and co-transfected, using Lipofectamine 2000 (Invitrogen), with pmXOR-EYFP and a pECFP-mBTN1A1 vector (0.15 μg, each), encoding either full-length ECFP-mBTN1A1 or deletion constructs (supplemental Table 1S). Cultures were incubated overnight, and the cells were then washed three times with KHM buffer (20 mM HEPES, pH 6.5, 110 mM potassium acetate, and 2 mM $MgCl_2$). Micrographs of selected cells were recorded using a Leica DMIRE2 fluorescence light microscope employing excitation wavelengths of 438 nm for ECFP and 500 nm for EYFP and separately visualizing the fluorophores between 426 and 450 nm and 488 and 512 nm, respectively. KHM buffer containing 20 μM digitonin was then added to permeabilize the plasma membrane. Soluble fluorescent fusion protein was allowed to diffuse out of the cells, and a second set of micrographs was recorded after there was no further change in the fluorescence signal (3–5 min). Transfection efficiencies were in the 50–70% range for each experiment, and ~90% of the doubly transfected cells in any one microscope field displayed the fluorescence patterns described.

Cell Fractionation and Detection of ECFP and EYFP Fusion Proteins—Control and transfected cells, as above, were suspended in 3 mM imidazole buffer, pH 7.4, containing 250 mM sucrose, 0.5 mM EDTA, and proteinase inhibitors, and mechanically disrupted by passage through a 27-gauge needle (10 times). The postnuclear supernatants were fractionated into membrane and cytosol fractions by centrifugation at 100,000 × g_{av} for 1 h and analyzed by Western blotting. Fusion proteins on the blots were detected with cross-reactive antibody to GFP (Invitrogen) diluted 1–2,500-fold, followed with a 1–10,000-fold dilution of goat anti-(rabbit IgG) horseradish peroxidase conjugate.

Immunoprecipitation—For immunoprecipitation from HEK 293T cells, cultures were grown in 10-cm dishes and transfected with a total of 12 μg of DNA using Lipofectamine 2000. Control and transfected cells were harvested in Dulbecco's PBS (Invitrogen) and the above proteinase inhibitors (PBS2) and mechanically disrupted by passage through a 27-gauge needle a total of 10 times. The nuclei were removed by centrifugation at 1,000 × g_{av} for 10 min at 4 °C, and the protein concentration of the postnuclear supernatants was adjusted to 2.4 mg/ml. RIPA buffer (2×) was then added so that the final concentrations of the constituents were protein 1.2 mg/ml, 50 mM Tris-HCl, pH 7.4, 40 mM NaCl, 1.0% (v/v) Nonidet P-40, 0.5% (w/v) sodium deoxycholate, and 0.1% (w/v) SDS. The mixtures were incubated at 4 °C with end-over-end stirring for 10 min, the detergent-soluble extracts were recovered by centrifugation at 16,000 × g_{av} for 5 min and then precleared by incubation with protein A-coated beads at 4 °C for 1 h (20 μl of beads per 1.2 ml of RIPA buffer extract). To ensure optimal precipitation of potential XOR-BTN1A1 complexes, protein A-Sepharose beads (GE Healthcare) were titrated with rabbit polyclonal antibody to mXOR to determine the minimum amount of antibody required to precipitate all of the XOR from the RIPA buffer extracts. Immunoprecipitates were collected on the beads by incubating 20 μl of optimally coated XOR-antibody/protein A beads with 1.0 ml of each RIPA buffer extract, overnight, at 4 °C with gentle agitation. The beads were then washed three times with ice-cold PBS2, and the bound protein was dissolved in SDS-PAGE buffer at 95 °C for 3 min and analyzed by SDS-PAGE and Western blotting. For immunoprecipitations from lactating mammary tissue, total membrane fractions were collected from the postnuclear supernatants of tissue homogenates as described under "Affinity Chromatography of Tissue Extracts on a Glutathione Matrix." After washing once with TBS, the microsomal membranes were extracted

with RIPA buffer, and the immunoprecipitations were conducted on the clarified RIPA buffer extracts essentially as described above for HEK 293T cells. The immunoprecipitations were repeated with total membrane fractions from three wild-type (*Btn1a1*$^{+/+}$) and three *Btn1a1*$^{-/-}$ C57/Bl6 mice, all at day 10 of lactation.

In Vitro Glutathione Bead Binding Assay for Protein-Protein Interactions—GST fusion proteins at final concentrations of 0.01–2 μM were bound to 0.2 ml (packed volume) of glutathione-coated beads in 0.5–1.0 ml of 50 mM Tris-HCl buffer, pH 7.4, for 3 h at 4 °C, and the beads were then washed three times with 1.0-ml aliquots of PBS. For the binding assays, the beads were divided into 20-μl portions and incubated overnight with XOR purified from bovine milk (bXO) (0.1–2 μM, monomeric M_r) in a total volume of 1.0 ml at 4 °C, with end-over-end stirring, in 1.5-ml Eppendorf tubes. The beads were then briefly washed three times with 1.0-ml aliquots of ice-cold PBS and heated to 95 °C in SDS-PAGE sample buffer. Aliquots of the centrifuged supernatants were analyzed by SDS-PAGE, together with known amounts of fusion protein and bXOR as standards (0.5–8 μg). Gels were stained with Coomassie Blue and destained in 10% (v/v) acetic acid, and amounts of fusion protein and bXOR in the samples were determined using Quantity One 1-D Analysis software (Bio-Rad). Binding was assayed either with constant amounts of fusion protein on the beads and increasing amounts of bXOR or with increasing amounts of fusion protein on the beads and saturating amounts of bXOR. Association and dissociation constants (K_A and K_D) were determined from the binding data by non-linear regression curve fit (hyperbola) using Prism version 5.0 software (Graphpad Software Inc.).

FPLC Gel Filtration—Proteins were separated by FPLC in a Superdex 200 HR prepacked column (1 × 30 cm) equilibrated with TBS, pH 7.4. For M_r estimations, the column was calibrated using the following protein standards; thyroglobulin (669,000), ferritin (440,000), aldolase (158,000), bovine serum albumin (67,000 and dimer), ovalbumin (43,000), chymotrypsinogen A (25,000), and ribonuclease A (13,700).

Electrophoresis and Western Blot—Techniques for electrophoresis and immunoblotting were essentially as described (31–33), using the ECL blotting kit according to the manufacturer's instructions (Amersham Biosciences/GE Healthcare). Antibodies to mouse (1) and bovine BTN1A1 (34) and bovine XOR (35) have been described previously. Rabbit anti-peptide antibodies to the C terminus of mouse XOR were prepared as described by Kreis (36) using the 21-mer peptide QFTTLCATGTPENCKSWSVRI (American Peptide, Sunnyvale, CA) as immunogen.

SPR—The binding of bXOR to GST fusion proteins in real time was evaluated by SPR using a Biacore 3000 Biosensor (GE Healthcare, Biacore, Uppsala, Sweden). Carboxymethyldextran sensor chips (CM5) in flow cells 1 and 2 were coated with 14000–15000 resonance units (RU) of monoclonal anti-GST antibody by standard amine coupling techniques according to the manufacturer's instructions (Biacore). GST fusion proteins were captured on the chips at a level of 50 RU by injecting an aliquot of GST alone (0.5 μg/ml) into flow cell 1, and GST fusion proteins (1.0 μg/ml) into flow cell 2, respectively, in HBS-EP buffer (10 mM HEPES, 150 mM NaCl, 3 mM EDTA, and 0.005% (v/v) surfactant p20, pH 7.4, filtered through a 0.2-μm filter and degassed before use). The kinetics of binding of bXOR to the immobilized GST fusion proteins were evaluated at a flow rate of 30 μl/min at 25 °C to minimize mass transport effects. bXOR at concentrations from 0 to 500 nM, in 60-μl aliquots, was injected into flow cells 1 and 2, and the association and dissociation rates were recorded for up to 6 min. To assess the effect of pH on binding kinetics, bXOR was diluted in HBS-EP buffer adjusted to pH 6.0, 6.5, 7.0, 7.4, or 8.0 with HCl or NaOH, and the association and dissociation analysis were performed as described above. The effect of salt on binding was similarly determined by using HBS-EP buffer containing variable amounts of NaCl. Chip surfaces were regenerated by removing GST proteins with 50-μl injections of 10 mM glycine-HCl buffer, pH 2.2. Sensorgrams were analyzed with BIAevaluation version 3.2 software (Biacore). Signals from the reference channel (GST) were subtracted from the channel containing GST fusion proteins to correct for refractive index changes, injection noise, and nonspecific binding to the reference surface. The signal obtained with a blank injection of HBS-EP buffer alone was then subtracted from the resulting data. Data were globally fitted to the Langmuir model for 1:1 binding and analyzed for significance by Student's *t* test.

CD Spectroscopy—Purified protein samples (0.5 mg/ml) were analyzed in a 0.2-mm cuvette using a π-180 spectrophotometer. Secondary structure was calculated using CDNN software (37), and extinction coefficients of proteins in native and denatured states were calculated, as described (38).

Mass Spectrometry—Proteins were digested in polyacrylamide gels with trypsin, and the peptide products were recovered following the procedure of Shevchenko *et al.* (39). Solubilized tryptic peptides from each band were analyzed by infusion electrospray ionization on a QStar Pulsar quadrupole-time-of-flight tandem mass spectrometer (Applied Biosciences, Foster City, CA). Molecular masses and tandem mass spectra of 1–5 peptides were used to search the NIHPD data base using the MASCOT search program (Matrix Science, London, UK). Peptide identification required probability scores exceeding 95%. The peptides identified from each band were used to identify the corresponding protein.

Assays—XOR for all of the binding studies was purified from bovine milk by the method of Sullivan *et al.* (35), omitting Triton X-100 from the electrofocusing step to ensure that variable traces of detergent did not compromise the binding assays. XOR in mouse milk lipid (MFGM and 100,000 × g_{av} soluble fractions) was assayed aerobically, in duplicate, in 100 mM sodium phosphate buffer, pH 7.2, containing 10% (v/v) dimethyl sulfoxide and 150 μM xanthine at 37 °C. The conversion of xanthine into uric acid was followed at 293 nm using a PerkinElmer Life Sciences Lambda 25 spectrophotometer. Enzyme activity (IU) was calculated using a molar extinction coefficient for uric acid under the assay conditions of 12.5 × 10^3 M^{-1} cm^{-1}. Protein was assayed by the bicinchoninic acid method of Smith *et al.* (40), using bovine serum albumin as a standard.

RESULTS

To directly explore potential interactions between BTN1A1 and XOR, we initially prepared the cytoplasmic domain of mouse BTN1A1 (mBTN1A1cyto) from yeast as a C-terminal fusion protein with GST (GST-mBTN1A1cyto) (supplemental Table 1S). Analysis by SDS-PAGE and two-dimensional gel electrophoresis showed that the purified protein was of the expected size (56,000) (supplemental Fig. 1S*a*) and focused as a series of isoelectric variants with pI values between 5.9 and 6.6 (supplemental Fig. 1S*b*) (the theoretical pI for GST-mBTN1A1cyto based on amino acid composition is 5.9). The CD spectrum of mBTN1A1cyto, obtained by subtracting the spectrum of GST from that of GST-mBTN1A1cyto, was consistent with a structure rich in β-sheets with no overt structural perturbations (supplemental Fig. 1S*c*) (16% α-helix, 35% antiparallel sheet, 8% parallel sheet, 17% β-turn, and 25% random coil). These values are consistent with a protein in which the B30.2 domain comprises about 75% of the total structure and is predicted to contain one or two α-helices and 13–15 β-strands (20, 21, 23).

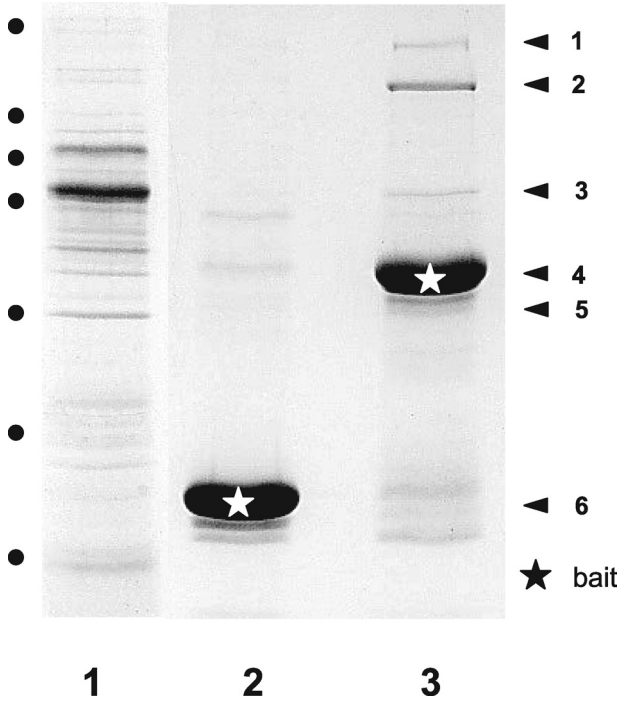

FIGURE 1. **Affinity chromatography of mammary proteins on GST-mBTN1A1cyto.** The postmicrosomal supernatant fraction from lactating mouse mammary tissue (3.0 ml; 50 mg of protein) was incubated with either GST or GST-mBTN1A1cyto bound to glutathione-agarose. Interacting proteins were then stripped from the columns using 10 mM glutathione. Samples (120 μg of protein/lane) were separated by electrophoresis in an 8% SDS-polyacrylamide gel. *Lane 1*, total postmicrosomal supernatant; *lane 2*, proteins bound to GST; *lane 3*, proteins bound to GST-mBTN1A1cyto. Representative results from one of three experiments are shown. *Proteins 1*, *2*, *3*, and *5* (*lane 3*) and *6* (*lane 2*) were identified by electrospray ionization mass spectrometry (Table 1). *Protein 4* (*lane 3*) was identified by Western blot. *Proteins 6* (*lane 2*) and *4* (*lane 3*) (*white asterisks*) are the baits, GST and GST-mBTN1A1cyto, respectively.

Using the purified and characterized GST-mBTN1A1cyto, we first asked which soluble proteins from lactating mouse mammary gland will bind to mBTN1A1cyto *in vitro*. Postmicrosomal supernatants obtained from the mammary glands of day 10 lactating mice (Fig. 1, *lane 1*) were fractionated on either GST or GST-mBTN1A1cyto immobilized on glutathione-agarose, and the bound proteins were eluted with glutathione. The control GST column failed to reproducibly pull down proteins from extracts, and hence only GST was detected after the glutathione wash (Fig. 1, *lane 2*; *protein 6*, *white asterisk*). Specifically bound proteins from the test column with approximate M_r of >200,000, 150,000, 66,000, and 50,000 were among the most prominent detected in the eluates by SDS-PAGE (Fig. 1, *lane 3*; *proteins 1–3* and *5*) together with GST-mBTN1A1cyto (Fig. 1, *lane 3*; *protein 4*, *white asterisk*). These proteins were identified as fatty acid synthase, XOR, serum albumin, and eukaryotic elongation factor γ1, respectively, based on peptide analysis by tandem mass spectrometry (Table 1). The 150-kDa protein, identified as XOR, was the most abundant. That GST-mBTN1A1cyto binds to XOR was confirmed by repeating the affinity chromatography with XOR purified from bovine milk (see further data below).

In order to identify the interactive region of mouse BTN1A1 that binds to XOR, we devised two assays, one in which fluorescent fusion proteins of mouse BTN1A1 and mouse XOR were expressed in HEK 293T cells and a second in which mutated GST-mBTN1A1cyto fusion proteins were bound to glutathione-coated beads and used in pull-down assays with bXOR.

For the *in vivo* cell expression assay, vectors were constructed encoding mouse BTN1A1 fused at the N terminus (after the signal sequence) to ECFP (pECFP-mBTN1A1) and mXOR fused at the C terminus to EYFP (pmXOR-EYFP) (supplemental Table 1S). When HEK 293T cells were separately transfected with these vectors, ECFP-mBTN1A1 was expressed and sorted to the plasma membrane (Fig. 2*A*, *a*) and a variable fraction to an intracellular site. This intracellular site appeared to be associated with or close to the *trans*-Golgi/*trans*-Golgi network, because co-expression of mBTN1A1-EYFP and the Golgi marker galactosyltransferase-ECFP showed close association of the two expressed proteins (supplemental Fig. 2S*A*). In contrast, mXOR-EYFP was expressed in the cytoplasm (Fig. 2*A*, *c*). Both expressed mBTN1A1 and mXOR fluorescent fusion proteins were of the expected size, with little evidence of degradation (shown by immunoblots of cell extracts probed with an antibody to GFP; supplemental Fig. 3S). That mXOR-EYFP

TABLE 1
Identification of proteins binding to mBTN1A1cyto by tandem mass spectrometry

Protein (see Fig.1)	Peptides identified	Protein identified	Calculated M_r
1	ALIAEATK, EAVLAAYWR, LTQGEVYK	Fatty acid synthase	272,653
2	FYLTVLQK, YENELSLR, TADELVFFVNGK IPAFGSIPTEFR, NADPETTLLAYLR	XOR	146,563
3	LSQTHPNADFAEITK	Serum albumin	66,659
5	ALIAAQYSGAQVR, TFLVGER	Elongation factor γ1	50,119
6	LLLEYLEEK, IEAIPQIDK	GST	25,498

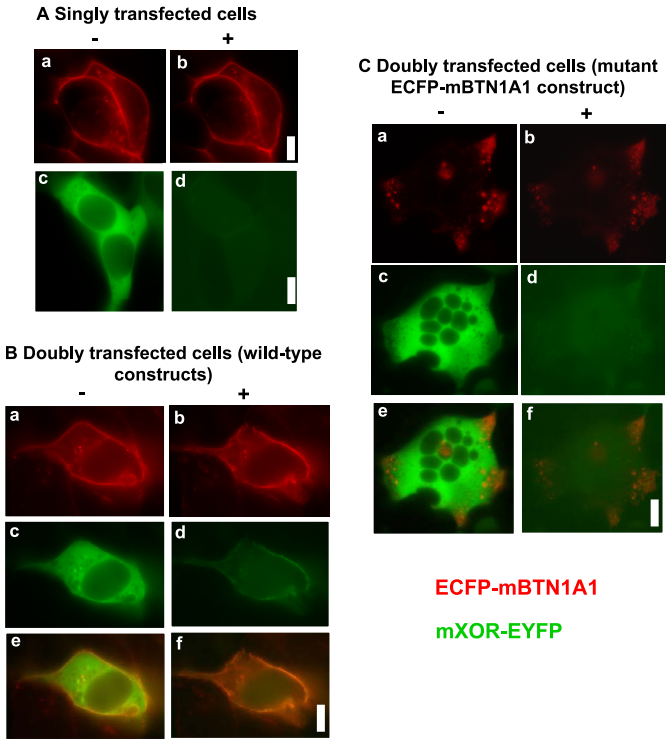

FIGURE 2. **Example of *in vivo* binding assay; expression of ECFP-mBTN1A1 and mXOR-EYFP in HEK 293T cells.** *A*, cells were transfected with either pECFP-mBTN1A1 (*a* and *b*) or pmXOR-EYFP (*c* and *d*) before (-) (*a* and *c*), and after (+) (*b* and *d*) treatment with digitonin. *B*, cells were co-transfected with pECFP-mBTN1A1 and pmXOR-EYFP. *a*, *c*, and *e*, before (−) treatment with digitonin; *b*, *d*, and *f*, after (+) treatment with digitonin. Shown is the fluorescence signal for ECFP-mBTN1A1 (*a* and *b*) and mXOR-EYFP (*c* and *d*). *e* and *f*, merged image. *C*, cells were co-transfected with pECFP-mBTN1A1$\Delta_{470-524}$ and pmXOR-EYFP before (−) (*a*, *c*, and *e*) and after (+) (*b*, *d*, and *f*) treatment with digitonin. Shown is the fluorescence signal for ECFP-mBTN1A1$\Delta_{470-524}$ (*a* and *b*) and mXOR-EYFP (*c* and *d*). *e* and *f*, merged image. *Bars*, 10 μm.

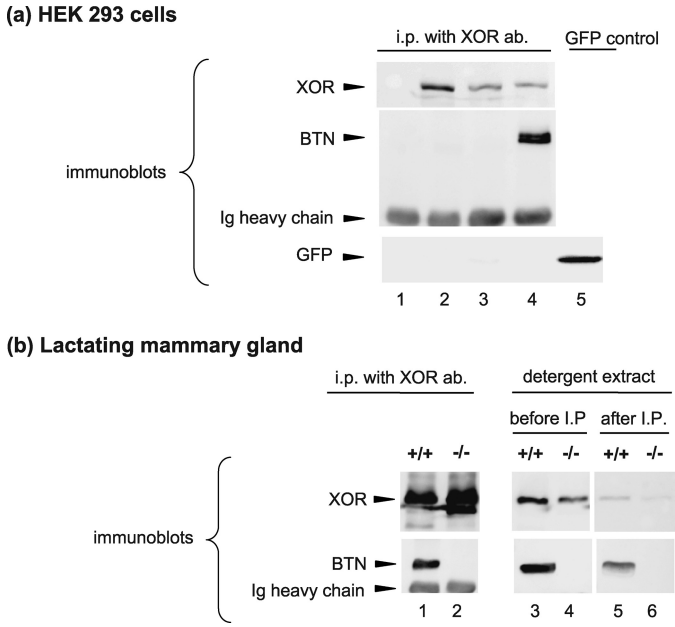

FIGURE 3. **Immunoprecipitation of BTN1A1-XOR complexes in HEK 293T cells and lactating mammary gland.** *a*, HEK 293T cells. Proteins were immunoprecipitated (*i.p.*) from RIPA buffer extracts with antibody to mXOR, separated by SDS-PAGE (6% gel), and first blotted with antibody to mBTN1A1 (*middle blot*). The blot was then stripped and reprobed with antibody to mXOR (*top blot*). Aliquots of the same immunoprecipitates were also separated by SDS-PAGE on a 10% gel to resolve GFP (*bottom blot*). Immunoprecipitates from non-transfected cells (*lane 1*), cells transfected with pmXOR-EYFP (*lane 2*), pmXOR-EYFP and a vector encoding GFP (*lane 3*), and pmXOR-EYFP and pECFP-mBTN1A1 (*lane 4*). The RIPA buffer extract used for the immunoprecipitation of mXOR-EYFP and GFP was separated in *lane 5* to validate the antibody to GFP (GFP control). *b*, lactating mammary gland. Proteins were immunoprecipitated from RIPA buffer extracts with antibody to mXOR, separated by SDS-PAGE (6% gel), and first blotted with antibody to mBTN1A1 (*bottom blot*). The blot was then stripped and reprobed with antibody to mXOR (*top blot*). Shown are immunoprecipitates from a wild-type mouse (*lane 1*) and a *Btn1a1*$^{-/-}$ mouse (*lane 2*). The corresponding RIPA buffer extracts, before and after incubation with the antibody-coated protein A beads, are shown for the wild-type mouse in *lanes 3* and *5* and for the *Btn1a1*$^{-/-}$ mouse in *lanes 4* and *6*, respectively. In both *a* and *b*, the blots shown are representative of one of three experiments each.

was primarily expressed in the cytoplasm was confirmed by treating the transfected cells with digitonin to permeabilize the cells and remove cytoplasmic proteins (41). Virtually all of the detectable mXOR-EYFP was washed out of the cells (Fig. 2*A*, compare *c* and *d*). As expected for a membrane protein, the distribution of ECFP-mBTN1A1 was unaffected by digitonin treatment (Fig. 2*A*, compare *a* and *b*).

To demonstrate binding between the two proteins, HEK 293T cells were co-transfected with both vectors. A fraction of the expressed mXOR-EYFP co-localized with ECFP-mBTN1A1 at the plasma membrane and in the Golgi region, even after treatment with digitonin (Fig. 2B and supplemental Fig. 2*SB*). That the two proteins were physically bound to each other was confirmed by immunoprecipitating clarified detergent extracts of transfected cells with antibody to mXOR (Fig. 3*a*). A specific band of protein, which reacted with antibody to mBTN1A1, was detected on blots of immunoprecipitates from doubly transfected cells (Fig. 3*a*, *lane 4*) but not from non-transfected control cells (Fig. 3*a*, *lane 1*), cells transfected only with mXOR-EYFP (Fig. 3*a*, *lane 2*), or cells doubly transfected with mXOR-EYFP and a vector encoding GFP (Fig. 3*a*, *lane 3*).

Mutated forms of ECFP-mBTN1A1 were then co-expressed with mXOR-EYFP, to determine which region of mBTN1A1cyto is required for localization of both proteins to cellular membranes. The cytoplasmic domain of BTN1A1 comprises three domains: a stem region closest to the membrane anchor, followed by a B30.2 domain and a C-terminal tail region (*schematic* in Fig. 4). Progressive deletion of the C-terminal region of ECFP-mBTN1A1cyto (supplemental Table 1S) showed that the entire tail domain could be deleted with no effect on binding to mXOR-EYFP (results summarized in Fig. 4). However, the removal of the most C-terminal 10 amino acids of the B30.2 domain resulted in relocation of the ECFP fusion protein to intracellular vesicles and abrogated binding to mXOR-EYFP (Figs. 2*C* and 4).

Binding between XOR and the cytoplasmic domain of BTN1A1 was confirmed by glutathione/GST pull-down assays. Fusion proteins of GST joined at the C terminus, either to mBTN1A1cyto or mutated forms of mBTN1A1cyto, were bound to glutathione-coated agarose beads and then incubated with a range of concentrations of bXOR. Binding of bXOR to GST-mBTN1A1cyto was saturable with apparent K_D values in the 50 nM range (Fig. 5*a* and Table 2). Deletion of the tail domain of mBTN1A1cyto had no influence on the binding of bXOR at saturating concentrations (Figs. 4 and 6*a*, compare

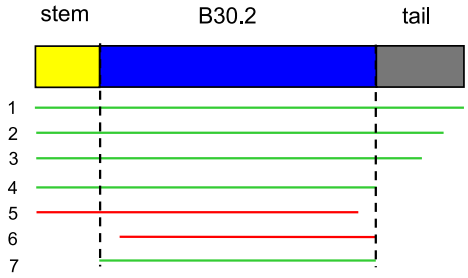

Construct	Deletion	Btn/XOR Binding? in transfected cells	in vitro
1	wild type	+[1]	+
2	Δ507-524	+	nd[2]
3	Δ493-524	+	+
4	Δ480-524	+	+
5	Δ470-524	-	-
6	Δ269-310; 480-524	nd	-
7	Δ269-285; 480-524	nd	+

[1] +, binding; -, no binding
[2] nd, not done

FIGURE 4. **Summary of bead binding and cell expression assays for interaction between mBTN1A1cyto and XOR.** Regions of mBTN1A1cyto that bound to XOR are indicated by *green lines*, and regions that did not bind are shown by *red lines*. Constructs indicated by *numbers* were inserted into either pECFP-C1 (Clontech) or pESP1 (Stratagene) as follows. For the cell expression assay, the vectors used (supplemental Table 1S) were pmXOR-EYFP in combination with pECFP-mBTN1A1 (*1*), pECFP-mBTN1A1 $\Delta_{507-524}$ (*2*), pECFP-mBTN1A1$\Delta_{493-524}$ (*3*), pECFP-mBTN1A1$\Delta_{480-524}$ (*4*), and pECFP-mBTN1A1$\Delta_{470-524}$ (*5*). For the *in vitro* bead binding assay, the vectors used were pGST-mBTN1A1cyto (*1*), pGST-mBTN1A1cyto$\Delta_{493-524}$ (*3*), pGST-mBTN1A1cyto$\Delta_{480-524}$ (*4*), pGST-mBTN1A1cyto$\Delta_{470-524}$ (*5*), pGST-mBTN1A1cyto$\Delta_{269-310;480-524}$ (*6*), and pGST-mBTN1A1cyto$\Delta_{269-285;\,480-524}$ (mB30.2) (*7*).

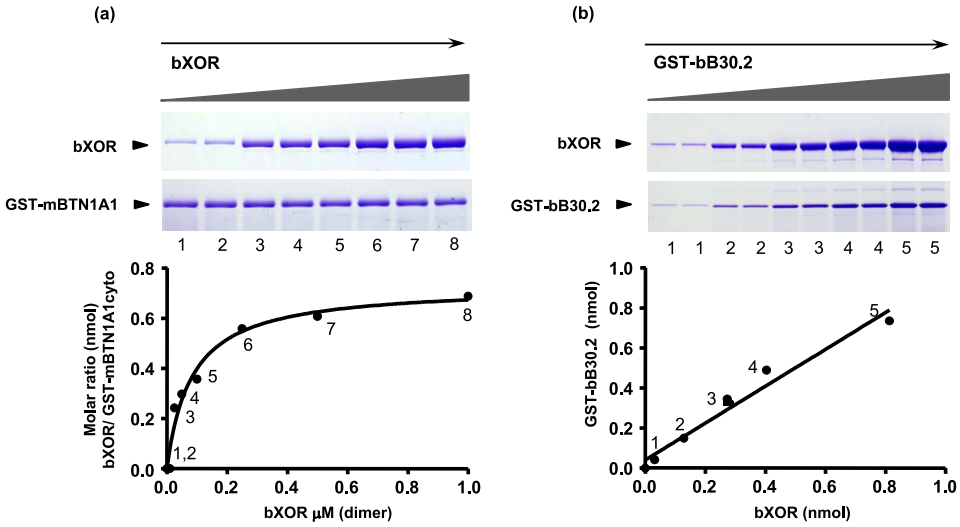

FIGURE 5. **Summary of bead binding assay for interaction between bXOR and BTN1A1.** *a*, example of binding between GST-mBTN1A1cyto (0.1 nmol) and increasing amounts of bXOR (0–1.0 μM dimer) to determine the K_D and stoichiometry at maximal binding; *b*, example of titration of GST-bB30.2 (0–0.8 nmol) and bXOR (1.0 nmol) to determine stoichiometry of binding. Densitometric data derived from the gels shown in the figure are plotted *below* each *panel*. Table 2 summarizes the binding data for GST-mBTN1A1cyto, GST-bBTN1A1cyto, and GST-bB30.2.

lanes 3 and *4*). GST-coated beads or uncoated beads served as controls (Fig. 6*a*, *lanes 1* and *2*). However, deletion of 10 amino acids from the C-terminal region of the B30.2 domain or deletion of 25 amino acids from the N-terminal region, abrogated binding (Fig. 6*a*, *lanes 5* and *6*). Most significantly, the B30.2 domain alone was sufficient for binding to bXOR (Figs. 4 and 6*a*, *lane 7*).

To investigate binding specificity within and across species, a series of GST fusion proteins were prepared that incorporated, at the C terminus, the entire cytoplasmic domains or the B30.2 domains of bovine and human BTN1A1 or the entire cytoplasmic domains of human BTN2A1 and BTN3A1. In addition, a protein comprising GST fused to the predicted B30.2 domain of human RoRet (TRIM 38) (42, 43) was prepared to test potential binding to a B30.2 domain in a protein outside of the BTN protein family. bXOR bound to the entire cytoplasmic domain or the B30.2 domain of BTN1A1 from mice (see above), cows, or humans (Fig. 6*b*, *lanes 1–3*) (data not shown). However, binding was limited to BTN1A1 subfamily members, since no interaction was detected between bXOR and BTN2A1, or BTN3A1 (Fig. 6*b*, *lanes 4* and *5*). Furthermore, bXOR did not bind to the B30.2 domain of human RoRet (TRIM 38) (Fig. 6*b*, *lane 6*; control in *lane 7*). These data demonstrate that XOR does not promiscuously bind to the B30.2 domains of even closely related paralogs of BTN1A1.

We next determined the affinity and kinetics of binding between XOR and BTN1A1 by SPR using GST fusion proteins encoding either bovine or mouse BTN1A1cyto domains as ligands and bXOR as analyte (Table 2 and Fig. 7*a*, example for GST-bBTN1A1cyto). Dissociation constants (K_D values) for GST-BTN1A1cyto from either species, determined at 25 °C, were not significantly different (average of 112 and 113 nM, for cow and mouse, respectively) and consistent with values in the 40–50 nM range for K_D values determined by the bead binding assay at 4 °C (Table 2). bXOR bound to GST-bB30.2 with statistically similar affinity (Table 2), confirming that the B30.2 domain is necessary and sufficient for maximal interaction between the two proteins. Binding was pH-dependent (determined either by SPR or the bead binding assay), with no binding detected below pH 6.0 (Fig. 7*b*), and binding affinities increased 5–7-fold when the salt concentration was lowered from 150 to 20 mM NaCl (Fig. 7*c*).

TABLE 2

Summary of binding characteristics for interaction between BTN fusion proteins and bXOR

K_D values within each assay are not significantly different ($p > 0.05$; MIXED procedure, version 9.1, SAS Institute (Cary, NC)). The number of determinations is shown in parentheses.

Parameter	Binding between bXOR and		
	GST-mBTN1A1cyto	GST-bBTN1A1cyto	GST-bB30.2
Dissociation constants (pH 7.4), K_D (nM)			
By bead binding assay	47 ± 35 (3)	50 ± 27 (3)	26 ± 14 (3)
By SPR	113 ± 6.4 (2)	112 ± 7.1 (2)	101 ± 31 (10)
Rate constants (pH 7.4)			
$k_a \times 10^{-4}$ M^{-1} s^{-1}	9.2 ± 2.4 (2)	7.4 ± 0.30 (2)	6.2 ± 1.3 (10)
$k_d \times 10^{-3}$ s^{-1}	10.4 ± 2.1 (2)	8.3 ± 0.15 (2)	6.0 ± 1.2 (10)
Binding stoichiometry (monomers) (BTN1A1:XOR::1.0:*x*)			
Binding curve	0.72 ± 0.03 (3)	0.79 ± 0.04 (3)	1.15 ± 0.32 (3)
Linear titration	0.35 ± 0.04 (2)	0.94 ± 0.18 (2)	1.15 ± 0.13 (2)

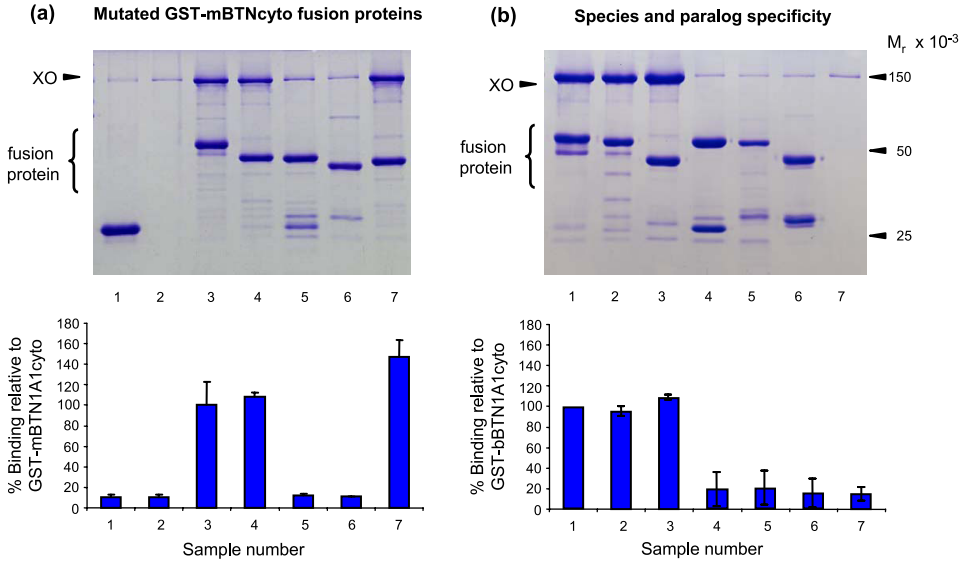

FIGURE 6. ***In vitro* bead binding assay for interaction between bXOR and wild-type or mutant mBTNs or BTNs from different species.** Each GST fusion protein (0.5 nmol) was bound to glutathione-coated beads (20-μl packed bed volume) and incubated with 0.5 nmol of bXOR in a final volume of 200 μl of PBS overnight at 4 °C. The beads were washed three times with PBS and heated in SDS-PAGE buffer for separation by SDS-PAGE. *a*, analysis of binding between bXOR and mutant forms of GST-mBTN1A1cyto. *Lane 1*, GST; *lane 2*, no protein; *lane 3*, GST-mBTN1A1cyto; *lane 4*, GST-mBTN1A1cytoΔ$_{480-524}$; *lane 5*, GST-mBTN1A1 cytoΔ$_{470-524}$; *lane 6*, GST-mBTN1A1cytoΔ$_{269-310;480-524}$; *lane 7*, GST-mBTN1A1cytoΔ$_{269-285;480-524}$ (mB30.2). *b*, specificity of binding between bXOR and different orthologs and paralogs of BTN. *Lane 1*, GST-bBTN1A1cyto; *lane 2*, GST-hBTN1A1cyto; *lane 3*, GST-hBTN1A1-B30.2; *lane 4*, GST-hBTN2A1cyto; *lane 5*, GST-hBTN3A1cyto; *lane 6*, GST-human RoRet(TRIM38)-B30.2; *lane 7*, no protein. Densitometric analysis of the results from three experiments (mean ± S.D.) are shown *below* each *panel*. Band densities are normalized (100%) to GST-mBTN1A1cyto (*lane 3*) in *a* and to GST-bBTN1A1cyto (*lane 1*) in *b*.

In order to determine the stoichiometry of binding between BTN1A1 and XOR, we titrated GST fusion proteins bound to glutathione-coated beads with bXOR, either keeping the amount of GST fusion protein constant and varying the amount of bXOR (binding curve) or varying the amount of GST fusion protein on the beads and adding saturating amounts of bXOR (linear titration) and then assaying for the amount of bXOR bound to the beads by quantitative densitometry (Fig. 5, *a* and *b*, and Table 2). Either approach gave BTN1A1/bXOR ratios consistent with equimolar binding (1.0:1.0), with the exception of the linear titration of GST-mBTN1A1cyto, which for unexplained reasons gave a ratio of 1.0:0.36. Binding was equimolar for both full-length mouse and bovine BTN1A1cyto or just the bB30.2 domain. Since bXOR is a homodimer (44), these data indicate that one XOR dimer binds to either two BTN1A1 monomers or one BTN1A1 dimer.

The oligomeric state of BTN1A1 and further estimates for stoichiometric ratios were investigated by gel filtration on Superdex 200 (FPLC) to determine the apparent M_r values of the purified proteins, separately, and together as BTN1A1-XOR complexes (Fig. 8 and Table 3). Both GST-mBTN1A1cyto and GST-bBTN1-A1cyto eluted as major peaks of protein with apparent M_r values in the range expected for tetramers (~190,000 and 215,000, respectively) (Table 3; see Fig. 8, *a* and *b*, *dotted blue lines*, for examples of GST-bBTN1A1cyto). Since GST is a dimer (45), we removed GST from GST-bBTN1A1cyto by digestion with thrombin to determine if the ability to oligomerize is an intrinsic property of BTN1A1cyto. The entire cytoplasmic domain of bBTN1A1, eluted with an apparent M_r of 48,000, ~80% of the mass expected for a dimer (61,020) (Fig. 8*b*, *dotted red line*, and Table 3). However, the purified bB30.2 domain eluted with an estimated M_r of 19,500, close to that expected for a monomer (23,437), with a lower amount of potential dimer partially separating as a shoulder on the major peak of protein (Fig. 8*b*, *solid red line*, and Table 3). These data are consistent with oligomerization of the fusion proteins to tetramers through separate dimeric interactions between the GST domains and dimeric interactions between the cytoplasmic domains of BTN1A1. Furthermore, interactions between the BTN molecules appear to be predominantly due to interactions within either the stem or tail regions, since the B30.2 domain was largely monomeric.

Complexes of the GST fusion proteins and bXOR, which had been prepared by binding and elution from glutathione-coated beads, eluted as broad peaks of protein with apparent M_r of ~500,000 with significant peak shoulders of ~800,000 (Table 3;

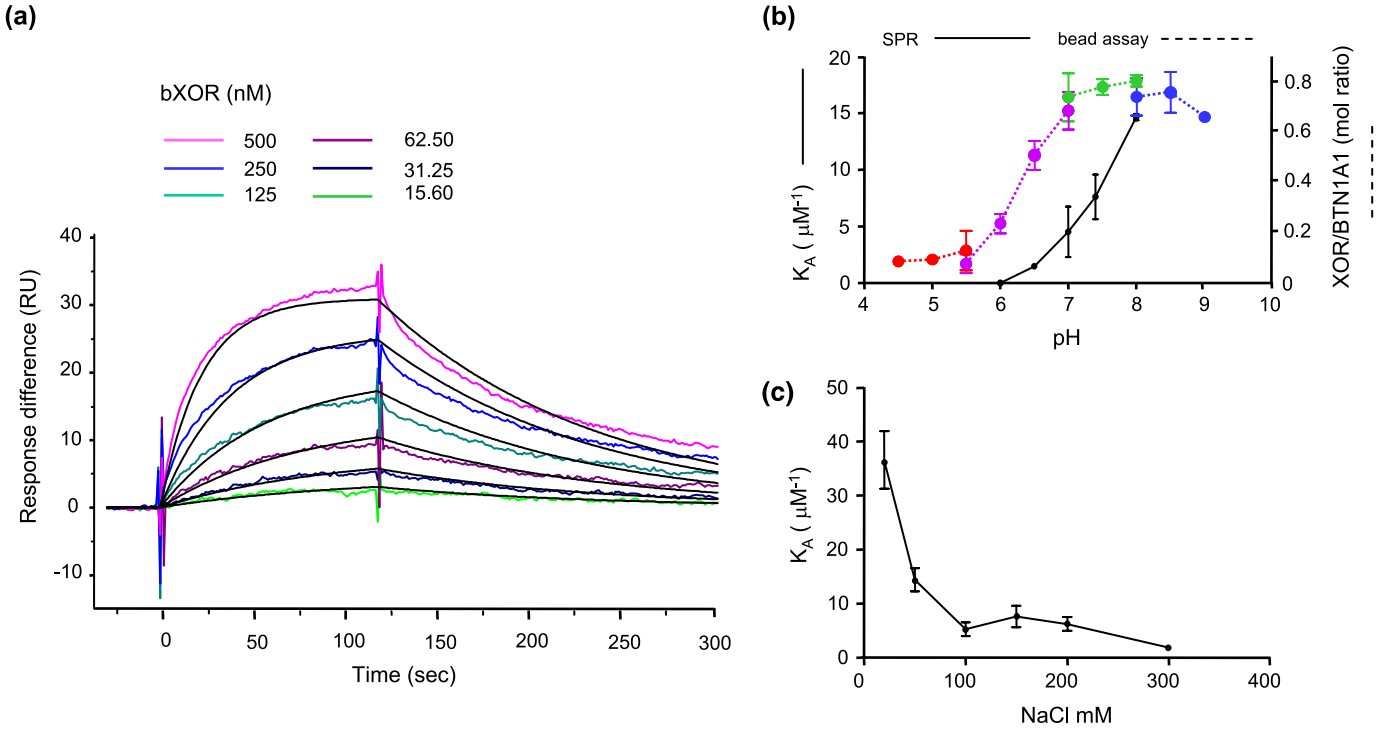

FIGURE 7. **Determination of equilibrium and kinetic rate constants for interaction between BTN1A1 proteins and bXOR by SPR.** *a*, representative example of the biosensor analysis of binding of bXOR to GST-bBTN1A1cyto (see Table 2 for complete summary). bXOR concentrations ranged from 15.6 to 500 nM, as shown in the figure. Data were fitted to the Langmuir model for 1:1 binding (*black lines*). *b*, effect of pH on binding of bXOR to GST-bB30.2. *Solid line*, SPR analysis (K_A μM^{-1}). *Dotted lines*, bead binding assay, using the following buffers: KH_2PO_4-KOH, pH 4.5–5.5 (*red*); MES, pH 5.5–7.0 (*purple*); HEPES, pH 7.0–8.0 (*green*); and Tricine, pH 8.0–9.0 (*blue*). *c*, effect of NaCl on the binding of bXOR to GST-bB30.2 (K_A μM^{-1}).

Fig. 8*a*, *solid black line*, example for GST-bBTN1A1). These data are consistent with stoichiometries of one tetrameric GST-fusion protein (M_r ~225,000) binding to either one or two dimers of XOR (expected M_r values for the complex of 520,000 and 815,000, respectively). To eliminate the confounding effects of dimeric GST, complexes of GST-bB30.2 and bXOR were prepared on glutathione-coated beads, and the GST was removed by digestion with thrombin. Such bB30.2-bXOR complexes eluted with an apparent M_r of 344 ± 13 (Fig. 8*c* and Table 3) (*i.e.* with a predicted monomeric bB30.2/XOR ratio of 1:0.85). Taken together, these data confirm that the cytoplasmic domain of BTN1A1 binds to bXOR in equimolar amounts via the B30.2 domain.

Finally, to assess the potential function of BTN1A1 and XOR in lactation, we first showed that the two proteins bind to each other *in vivo*. Detergent extracts of membrane fractions, prepared from the lactating mammary tissue of either wild type (*Btn1a1*$^{+/+}$) or "knock-out" (*Btn1a1*$^{-/-}$) mice, were immunoprecipitated with antibody to mXOR. A band of protein that reacted with antibody to mBTN1A1 was detected when the immunoprecipitates from wild-type mice were analyzed by Western blot using antibody to mBTN1A1 (Fig. 3*b*, *lane 1*), whereas there was no reaction with immunoprecipitates from *Btn1a1*$^{-/-}$ mice (Fig. 3*b*, *lane 2*). ~37.5 ± 6.2% of BTN1A1 (mean and S.D. of three determinations) was bound to XOR, as determined by densitometric analysis of the detergent extracts before and after incubation with the antibody-coated protein A beads (Fig. 3*b*, *lanes 3* and *5*). Interestingly, XOR was recovered in the immunoprecipitates from knock-out mice, indicating that XOR binds to membranes in the absence of BTN1A1 (Fig. 3*b*, *lane 2*).

To determine whether the binding of XOR to BTN1A1 has relevance to the potential function of these proteins in milk lipid secretion, we compared the association of XOR with lipid droplets in the presence and absence of BTN1A1 using wild-type, heterozygous (*Btn1a1*$^{+/-}$), or *Btn1a1*$^{-/-}$ mice. No significant differences in the amount of XOR relative to total protein (determined by immunoblot) or activity (determined as xanthine oxidase activity) were detected in lipid droplets from the milks of wild-type, *Btn1a1*$^{+/-}$, or *Btn1a1*$^{-/-}$ mice (Fig. 9). However, although the levels of XOR were comparable between wild-type and *Btn1a1*$^{-/-}$ mice, there was a highly significant difference in the amount of XOR that remained bound to the MFGM compared with the amount of XOR that was released in a soluble form when membrane was stripped from the core lipid by freeze-thawing the cream samples. Approximately four times as much XOR remained bound to membrane compared with the soluble fraction in wild-type mice, whereas a majority of the XOR in both *Btn1a1*$^{+/-}$ and *Btn1a1*$^{-/-}$ mice was released into the soluble fraction (Fig. 9, *b* and *c*). Furthermore, a fraction of the membrane-bound XOR in wild-type mice separated as aggregates when samples were separated by SDS-PAGE, compared with fractions from *Btn1a1*$^{-/-}$ mice (*bracket* in Fig. 9*a*, *i*). At least some of these aggregates may consist of complexes of XOR and BTN1A1, because both proteins were detected in the same protein bands by stripping the immunoblots and reprobing them with an antibody to BTN1A1; *filled circle* in Fig. 9*a*, *ii*). Thus, XOR is incorporated into secreted

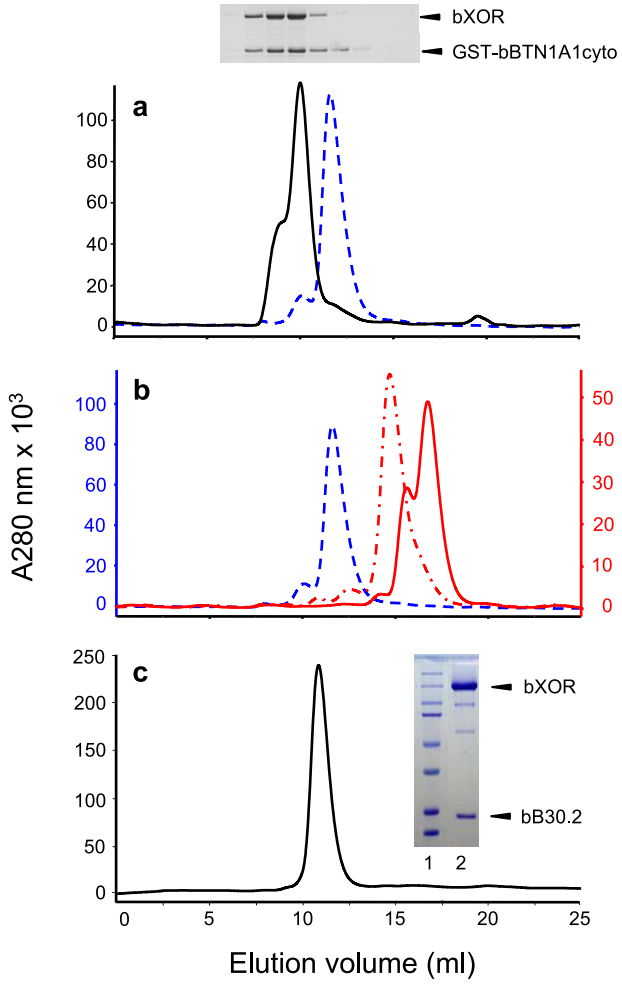

FIGURE 8. **Gel filtration of protein complexes.** Samples were separated by FPLC on a 1 × 30-cm column of Superdex 200 in TBS, pH 7.4, and protein was detected at $A_{280\ nm}$ (light path, 0.5 cm). *a*, GST-bBTN1A1cyto (10 nmol) (*dotted blue line*) and GSTbBTN1A1-bXOR complex (10 nmol) (*black line*). The *gel inset* shows analysis of peak fractions by SDS-PAGE; *b*, GST-bBTN1A1cyto (8 nmol) (*dotted blue line*), bBTN1A1cyto (8 nmol) (*dotted red line*), and bB30.2 (8 nmol) (*solid red line*). *c*, GSTbB30.2-bXOR complex; *gel inset* shows analysis of peak fraction by SDS-PAGE (*lane 2*) in comparison with protein standards (from *top* to *bottom*, 250, 150, 100, 75, 50, 37, 25, and 20 kDa; *lane 1*).

TABLE 3

Protein M_r values estimated by gel filtration on Superdex 200

Figures in boldface type indicate the most abundant species. Values in parentheses indicate the number of determinations, and values in square brackets indicate the approximate M_r of proteins within a prominent shoulder associated with a major peak. ND, not done.

Protein	$M_r \times 10^{-3}$	
	Mouse	Cow
GST-BTN1A1cyto; M_r expected for monomer	**189 ± 19** (5); 55.92	**216 ± 4.2** (3); 56.51
BTN1A1cyto; M_r expected for monomer	ND	**48 ± 3.1** (3); 30.51
B30.2; M_r expected for monomer	ND	[30.8], **19.5** (1); 23.44
GST-BTN1A1cyto-bXOR complex	[764 ± 33] (5) **496 ± 29**	[807 ± 10] (3) **528 ± 8**
B30.2-bXOR complex	ND	**344 ± 13** (3)

lipid droplets in the absence of BTN1A1 but is more loosely bound to the MFGM. These data are consistent with the possibility that association of XOR with the MFGM is stabilized by binding to the cytoplasmic domain of BTN1A1, but XOR is initially incorporated into lipid droplets by another mechanism.

DISCUSSION

The data described firmly establish that the cytoplasmic domain of BTN1A1 binds to XOR *in vivo* and *in vitro* with relatively high affinity and in a salt- and pH- dependent manner via the B30.2 domain. Binding is stoichiometric with predicted ratios of one XOR homodimer bound to two BTN monomers or one BTN1A1 dimer. Furthermore, binding is independent of species; bovine or mouse XOR binds to the B30.2 domain of mouse, cow, or human BTN1A1. No binding was detected between XOR and even the closely related paralogs, BTN2A1 and BTN3A1, or to the B30.2 domain of the otherwise unrelated RoRet (TRIM 38) protein. Analysis of *Btn1a1*$^{-/-}$ mice showed that expression of BTN1A1 is required for the stable association of XOR with the MFGM *in vivo*. These data provide novel insights into the potential roles of BTN1A1 and XOR in milk lipid secretion, the relationship between BTN1A1 and other family members, and the possible functions of BTN1A1 in other cellular contexts.

Based on available structural data, there is an emerging consensus that the B30.2 domain serves as a universal protein binding module (20–24, 46). The B30.2 domain is widely distributed throughout the proteome (25, 47, 48), occurring within and outside of the BTN protein family and the immune system. The most conserved region of the domain comprises a core β-sandwich, with variable loops linking adjoining β-strands. In all B30.2 domain structures that have been characterized with bound ligand (21–23), the interacting partner binds, via hydrogen bonding and hydrophobic interactions, to one or more discrete pockets formed from the variable loops. Comparison of the linear sequences of these B30.2 domains with those of BTN1A1 and other family members (BTN2A1, BTN2A2, BTN2A3, BTN3A1, BTN3A2, and BTN3A3) reveals a similar predicted pattern of conserved β-strands and variable loops (21, 23). XOR is therefore likely to interact with BTN1A1 through analogous binding motifs, which are not conserved in BTN2A1 or BTN3A1 (Fig. 6*b*). Similar binding characteristics are also to be expected because of similarities in the dissociation constants (K_D values) for the binding of ligand to BTN1A1 (27 nM in 20 mM NaCl), GUSTAVUS (40 nM in 150 mM NaCl) (21), and TRIM 21 (37 nM in 50 mM NaCl) (23) and the lower K_D values (higher affinities) determined at lower salt concentrations (Fig. 7*c*) (23). However, because of the presumed discontinuous nature of binding motifs in the linear sequence, it is not possible to predict which residues in BTN1A1 function in binding. Resolution of these structural issues will require analysis by x-ray crystallography.

In vitro bead binding assays showed that bXOR binds to the B30.2 domain of BTN1A1 in a monomeric ratio of 1:1 (Fig. 5 and Table 2), which is in agreement with a global best fit of the SPR data using the 1:1 Langmuir model for binding (Fig. 7*a*, *black lines*). These data are also consistent with ligand binding ratios for other B30.2 domain-containing proteins, including GUSTAVUS and TRIM21 (21, 23). Since bXOR is a homodimer (44), a maximum of two B30.2 domains are predicted to bind to one native XOR molecule. *In vitro* analysis by FPLC showed that bBTN1A1cyto can form dimers. Dimerization is most likely through the stem region, which is predicted to have

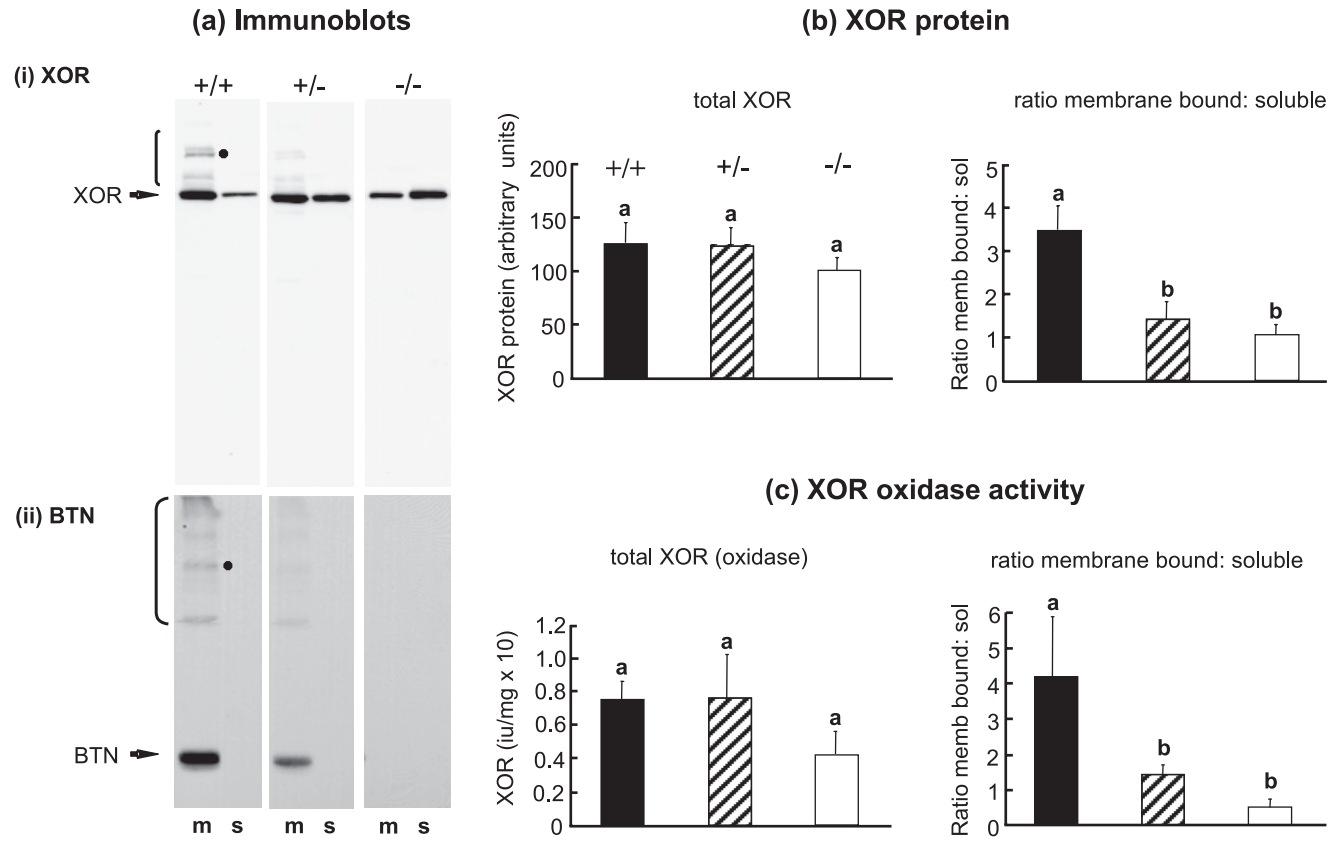

FIGURE 9. **Distribution and amount of XOR in milk lipid droplets and MFGM fractions from *Btn1a1*$^{+/+}$, *Btn1a1*$^{+/-}$, and *Btn1a1*$^{-/-}$ mice at peak lactation.** Milk lipid fractions were separated into membrane-bound and soluble fractions as described under "Experimental Procedures" and analyzed by Western blot (*a* and *b*) and an enzyme assay (*c*). *a* (*i*), membrane-bound (*m*) and soluble (*s*) XOR detected by Western blot. *a* (*ii*), the same immunoblots from *a* (*i*), stripped and reprobed with an antibody to mouse BTN1A1. Aggregates of XOR and BTN1A1 are indicated by *brackets* in *i* and *ii*, respectively, and potential complexes of XOR and BTN1A1 are shown by *filled circles*. *b*, *left*, comparative amounts of total XOR determined by densitometry of stained immunoblots; *right*, ratio of membrane-bound to soluble XOR. *c*, *left*, comparative amounts of total XOR activity; *right*, ratio of membrane-bound to soluble XOR activity. For each genotype, milk lipid samples from three mice on day 10 of lactation were analyzed in duplicate. Data within each *panel* with *different letters* are significantly different from each other ($p < 0.05$) using Student-Newman-Keul's multiple comparison test.

α-helical character, since the B30.2 domain was largely monomeric (Fig. 8*b*), and the cytoplasmic tail domain is probably disordered because of intermittent P residues (GlobPlot™ prediction). Therefore, XOR has the potential to bind either one or two BTN1A1 monomers or one dimer in a pH-dependent manner.

These binding data are relevant to several potential functions of BTN1A1 *in vivo*. In the context of milk lipid secretion, fat droplets are coated with apical membrane as they are expelled from mammary cells, and the resulting MFGM in many species contains large amounts of BTN1A1 and XOR (2, 49, 50). The observation that XOR only binds to BTN1A1, the BTN family member that is highly expressed in the lactating mammary gland, and not to other BTN paralogs provides further evidence that these two proteins function together in lactation. At least two models have been proposed to explain how BTN1A1 and XOR may function in lipid secretion (2, 28, 51).

In one model, BTN1A1 as a transmembrane protein binds to XOR, which serves as a linker protein to other proteins on the lipid droplet surface, including adipophilin (2). Concerted interactions between such BTN-XOR complexes and homophilic adhesive interactions between BTN1A1 molecules are proposed to proceed as a wave around the droplet and lead to the uniform coating of the droplet with membrane and to the eventual expulsion of the lipid droplet from the cell. At some point during or after secretion, associations between BTN1A1 and XOR culminate in formation of a characteristic protein coat complex that can be identified by freeze-etch electron microscopy (52, 53). Knock-out of BTN1A1 expression in *Btn1a1*$^{-/-}$ mice (1) or reduction of the amount of XOR in one strain of Xdh$^{+/-}$ mice (27) eliminates or reduces the possibility of interactions between BTN1A1 and XOR, leading to the secretion of abnormally large and unstable lipid droplets. Thus, BTN1A1 is seen to function as a transmembrane scaffold, which binds to XOR and other proteins on the droplet surface to ensure the coordinated and regulated secretion of lipid droplets into milk.

The binding data from this current study confirm that BTN1A1, through interactions with the B30.2 domain, binds with high affinity to XOR and that BTN1A1 molecules can bind to each other. However, the observation that XOR is secreted with lipid droplets in the absence of BTN1A1 (Fig. 9) is not compatible with the proposal that BTN1A1 directly recruits XOR into the lipid droplet (2) and suggests that XOR is initially recruited into the MFGM by other means (*e.g.* by being carried to the apical plasma membrane on the surface of intracellular lipid droplets independently of BTN1A1 or by binding to other proteins as well as BTN1A1) (see Refs. 51 and 54 for discussion).

Interestingly, XOR was recovered in crude membrane fractions (Fig. 3*b*, *lane 4*) and the MFGM (Fig. 9*a*, *i*) in the absence of BTN1A1, indicating that XOR can bind to other membrane components. However, such associations may be artifactually induced *in vitro*, because XOR has the potential to bind to glycoaminoglycans on exoplasmic membrane surfaces (55) when it is released into the soluble phase from total cell lysates or homogenized milk lipid droplets. Whatever the case, at some point during the secretion process, association of XOR with the MFGM becomes *dependent* on the presence of BTN1A1, because its elimination in null mice leads to the release of a substantial amount of soluble XOR from isolated milk lipid globules (Fig. 9). A full description of how the MFGM is assembled will require the application of live cell imaging techniques, more refined analysis of the distribution of XOR and BTN1A1 in secretory epithelial cells, and identification of additional protein binding partners and regulatory molecules. Such additional proteins may include fatty acid synthetase, the γ-subunit of elongation factor 1 (Table 1), and other GTP-binding proteins (56).

In a second model, based on freeze-fracture labeling techniques, Robenek *et al.* (28) proposed that secretion of lipid droplets is solely mediated by adhesive interactions between BTN1A1 molecules in the apical plasma membrane and BTN1A1 molecules on the lipid droplet surface and that XOR plays no role at any stage, because it does not colocalize with BTN1A1 in the freeze-fractured faces of secreted lipid droplets. This model is not consistent with the data in this paper showing that BTN1A1 binds tightly to XOR and that the association of XOR with the MFGM is dependent upon the presence of BTN1A1 (Fig. 9). Furthermore, it is inconsistent with the data of McManaman *et al.* (54) showing that at least a fraction of BTN1A1 may bind to XOR by disulfide bonds in isolated MFGM. Also, the model assumes that BTN1A1, which is an integral membrane protein, binds with unconventional topology to the phospholipid monolayer surrounding cytoplasmic lipid droplets.

Historically, BTN1A1 has been considered to be a mammary-specific protein (15), and its functions have been thought to be limited to potential roles in milk lipid secretion, a process unique to the mammary gland (2). However, extensive tissue surveys by more sensitive histochemical (BTN1A1 on the Human Protein Atlas site on the World Wide Web) and reverse transcription-PCR techniques[6] indicate that BTN1A1 is expressed in other cells and tissues, including spleen, thymus, esophagus, and lymphoid cells in the tonsil. Since none of these other tissues secrete membrane-coated lipid droplets, BTN1A1 must function in other capacities. Two possibilities deserve special consideration. First, BTN1A1 and its binding partner, XOR, possess all of the hallmarks of a novel signaling system; BTN1A1 is an integral protein with IgG folds in the exoplasmic domain, which could bind ligand, and a cytoplasmic B30.2 domain, which binds XOR in a pH-dependent manner (this study). In the appropriate physiological contexts, XOR, either as a dehydrogenase or an oxidase may generate short lived reactive species, including H_2O_2, superoxide radical, and NO, which may act on downstream targets and regulate gene expression (57). Second, BTN1A1 and XOR (58, 59) may function as components of the innate immune system by generating antibacterial reactive oxygen and nitrogen species following engagement of BTN1A1 with immune receptors or bacterial surfaces. In this context, milk contains large numbers of exosomes, small immunoregulatory 30–100-nm vesicles that contain significant amounts of both BTN1A1 and XOR (60), which may serve to protect the lactating mammary gland from bacterial pathogens.

The SPRY and B30.2 domains have been identified in at least 86 human genes (25). In other organisms, well over 2,000 sequences encoding B30.2, SPRY, and PRY domains have been cataloged, including several hundred NOD-like immune receptors in teleost fish (48). Although XOR only bound to the B30.2 domain of BTN1A1 in our limited survey of potential binding partners, a more extensive screen is warranted, to determine whether XOR binds to the B30.2 domain in other proteins within and outside of the immune system.

Acknowledgments—We thank Drs. Jennifer Lippincott-Schwartz and Dale Hailey (National Institutes of Health, Bethesda, MD) for modified Clontech vectors encoding monomerized forms of ECFP and EYFP and galactosyltransferase-ECFP and Dr. David Rhodes (University of Cambridge, UK) for cDNAs encoding hBTN2A1, hBTN3A1, and human RoRet. Dr. Yinghua Zhang (University of Maryland Medical School, Baltimore, MD) conducted the SPR spectroscopy on a fee for service basis, and Drs. Philip Bryan (Center for Advanced Research in Biotechnology, Gaithersburg, MD) and Victor Munoz (Department of Chemistry and Biochemistry, University of Maryland, College Park, MD) provided help and advice with the CD spectroscopy. Liane Langbehn provided animal care and helped with the preparation of rabbit antibody to bXOR.

REFERENCES

1. Ogg, S. L., Weldon, A. K., Dobbie, L., Smith, A. J., and Mather, I. H. (2004) *Proc. Natl. Acad. Sci. U.S.A.* **101,** 10084–10089
2. Mather, I. H., and Keenan, T. W. (1998) *J. Mammary Gland Biol. Neoplasia* **3,** 259–273
3. Valentonyte, R., Hampe, J., Huse, K., Rosenstiel, P., Albrecht, M., Stenzel, A., Nagy, M., Gaede, K. I., Franke, A., Haesler, R., Koch, A., Lengauer, T., Seegert, D., Reiling, N., Ehlers, S., Schwinger, E., Platzer, M., Krawczak, M., Müller-Quernheim, J., Schürmann, M., and Schreiber, S. (2005) *Nat. Genet.* **37,** 357–364
4. Nguyen, T., Liu, X. K., Zhang, Y., and Dong, C. (2006) *J. Immunol.* **176,** 7354–7360
5. Arnett, H. A., Escobar, S. S., Gonzalez-Suarez, E., Budelsky, A. L., Steffen, L. A., Boiani, N., Zhang, M., Siu, G., Brewer, A. W., and Viney, J. L. (2007) *J. Immunol.* **178,** 1523–1533
6. Boyden, L. M., Lewis, J. M., Barbee, S. D., Bas, A., Girardi, M., Hayday, A. C., Tigelaar, R. E., and Lifton, R. P. (2008) *Nat. Genet.* **40,** 656–662
7. Stefferl, A., Schubart, A., Storch, M., Amini, A., Mather, I., Lassmann, H., and Linington, C. (2000) *J. Immunol.* **165,** 2859–2865
8. Guggenmos, J., Schubart, A. S., Ogg, S., Andersson, M., Olsson, T., Mather, I. H., and Linington, C. (2004) *J. Immunol.* **172,** 661–668
9. Mañá, P., Goodyear, M., Bernard, C., Tomioka, R., Freire-Garabal, M., and Liñares, D. (2004) *Int. Immunol.* **16,** 489–499
10. Gardinier, M. V., Amiguet, P., Linington, C., and Matthieu, J. M. (1992) *J. Neurosci. Res.* **33,** 177–187
11. Linsley, P. S., Peach, R., Gladstone, P., and Bajorath, J. (1994) *Protein Sci.* **3,** 1341–1343

[6] I. A. Smith, B. R. Knezevic, J. Ammann, D. A. Rhodes, D. Aw, D. B. Palmer, I. H. Mather, and J. Trowsdale, unpublished observations.

12. Vernet, C., Boretto, J., Mattéi, M. G., Takahashi, M., Jack, L. J., Mather, I. H., Rouquier, S., and Pontarotti, P. (1993) *J. Mol. Evol.* **37,** 600–612
13. Ponting, C., Schultz, J., and Bork, P. (1997) *Trends Biochem. Sci.* **22,** 193–194
14. Jack, L. J., and Mather, I. H. (1990) *J. Biol. Chem.* **265,** 14481–14486
15. Franke, W. W., Heid, H. W., Grund, C., Winter, S., Freudenstein, C., Schmid, E., Jarasch, E. D., and Keenan, T. W. (1981) *J. Cell Biol.* **89,** 485–494
16. Harpaz, Y., and Chothia, C. (1994) *J. Mol. Biol.* **238,** 528–539
17. Breithaupt, C., Schubart, A., Zander, H., Skerra, A., Huber, R., Linington, C., and Jacob, U. (2003) *Proc. Natl. Acad. Sci. U. S. A.* **100,** 9446–9451
18. Malcherek, G., Mayr, L., Roda-Navarro, P., Rhodes, D., Miller, N., and Trowsdale, J. (2007) *J. Immunol.* **179,** 3804–3811
19. Compte, E., Pontarotti, P., Collette, Y., Lopez, M., and Olive, D. (2004) *Eur. J. Immunol.* **34,** 2089–2099
20. Grütter, C., Briand, C., Capitani, G., Mittl, P. R., Papin, S., Tschopp, J., and Grütter, M. G. (2006) *FEBS Lett.* **580,** 99–106
21. Woo, J. S., Imm, J. H., Min, C. K., Kim, K. J., Cha, S. S., and Oh, B. H. (2006) *EMBO J.* **25,** 1353–1363
22. Woo, J. S., Suh, H. Y., Park, S. Y., and Oh, B. H. (2006) *Mol. Cell* **24,** 967–976
23. James, L. C., Keeble, A. H., Khan, Z., Rhodes, D. A., and Trowsdale, J. (2007) *Proc. Natl. Acad. Sci. U.S.A.* **104,** 6200–6205
24. Kuang, Z., Yao, S., Xu, Y., Lewis, R. S., Low, A., Masters, S. L., Willson, T. A., Kolesnik, T. B., Nicholson, S. E., Garrett, T. J., and Norton, R. S. (2009) *J. Mol. Biol.* **386,** 662–674
25. Rhodes, D. A., de Bono, B., and Trowsdale, J. (2005) *Immunology* **116,** 411–417
26. Ishii, T., Aoki, N., Noda, A., Adachi, T., Nakamura, R., and Matsuda, T. (1995) *Biochim. Biophys. Acta* **1245,** 285–292
27. Vorbach, C., Scriven, A., and Capecchi, M. R. (2002) *Genes Dev.* **16,** 3223–3235
28. Robenek, H., Hofnagel, O., Buers, I., Lorkowski, S., Schnoor, M., Robenek, M. J., Heid, H., Troyer, D., and Severs, N. J. (2006) *Proc. Natl. Acad. Sci. U.S.A.* **103,** 10385–10390
29. Ohtsubo, T., Rovira, II, Starost, M. F., Liu, C., and Finkel, T. (2004) *Circ. Res.* **95,** 1118–1124
30. Wood, V., Gwilliam, R., Rajandream, M. A., Lyne, M., Lyne, R., Stewart, A., Sgouros, J., Peat, N., Hayles, J., Baker, S., Basham, D., Bowman, S., Brooks, K., Brown, D., Brown, S., Chillingworth, T., Churcher, C., Collins, M., Connor, R., Cronin, A., Davis, P., Feltwell, T., Fraser, A., Gentles, S., Goble, A., Hamlin, N., Harris, D., Hidalgo, J., Hodgson, G., Holroyd, S., Hornsby, T., Howarth, S., Huckle, E. J., Hunt, S., Jagels, K., James, K., Jones, L., Jones, M., Leather, S., McDonald, S., McLean, J., Mooney, P., Moule, S., Mungall, K., Murphy, L., Niblett, D., Odell, C., Oliver, K., O'Neil, S., Pearson, D., Quail, M. A., Rabbinowitsch, E., Rutherford, K., Rutter, S., Saunders, D., Seeger, K., Sharp, S., Skelton, J., Simmonds, M., Squares, R., Squares, S., Stevens, K., Taylor, K., Taylor, R. G., Tivey, A., Walsh, S., Warren, T., Whitehead, S., Woodward, J., Volckaert, G., Aert, R., Robben, J., Grymonprez, B., Weltjens, I., Vanstreels, E., Rieger, M., Schäfer, M., Müller-Auer, S., Gabel, C., Fuchs, M., Düsterhöft, A., Fritzc, C., Holzer, E., Moestl, D., Hilbert, H., Borzym, K., Langer, I., Beck, A., Lehrach, H., Reinhardt, R., Pohl, T. M., Eger, P., Zimmermann, W., Wedler, H., Wambutt, R., Purnelle, B., Goffeau, A., Cadieu, E., Dreano, S., Gloux, S., Lelaure, V., Mottier, S., Galibert, F., Aves, S. J., Xiang, Z., Hunt, C., Moore, K., Hurst, S. M., Lucas, M., Rochet, M., Gaillardin, C., Tallada, V. A., Garzon, A., Thode, G., Daga, R. R., Cruzado, L., Jimenez, J., Sanchez, M., del Rey, F., Benito, J., Dominguez, A., Revuelta, J. L., Moreno, S., Armstrong, J., Forsburg, S. L., Cerutti, L., Lowe, T., McCombie, W. R., Paulsen, I., Potashkin, J., Shpakovski, G. V., Ussery, D., Barrell, B. G., and Nurse, P. (2002) *Nature* **415,** 871–880
31. Laemmli, U. K. (1970) *Nature* **227,** 680–685
32. Neira, L. M., and Mather, I. H. (1990) *Protoplasma* **159,** 168–178
33. Towbin, H., Staehelin, T., and Gordon, J. (1979) *Proc. Natl. Acad. Sci. U.S.A.* **76,** 4350–4354
34. Banghart, L. R., Chamberlain, C. W., Velarde, J., Korobko, I. V., Ogg, S. L., Jack, L. J., Vakharia, V. N., and Mather, I. H. (1998) *J. Biol. Chem.* **273,** 4171–4179
35. Sullivan, C. H., Mather, I. H., Greenwalt, D. E., and Madara, P. J. (1982) *Mol. Cell Biochem.* **44,** 13–22
36. Kreis, T. E. (1986) *EMBO J.* **5,** 931–941
37. Böhm, G., Muhr, R., and Jaenicke, R. (1992) *Protein Eng.* **5,** 191–195
38. Gill, S. C., and von Hippel, P. H. (1989) *Anal. Biochem.* **182,** 319–326
39. Shevchenko, A., Wilm, M., Vorm, O., and Mann, M. (1996) *Anal. Chem.* **68,** 850–858
40. Smith, P. K., Krohn, R. I., Hermanson, G. T., Mallia, A. K., Gartner, F. H., Provenzano, M. D., Fujimoto, E. K., Goeke, N. M., Olson, B. J., and Klenk, D. C. (1985) *Anal. Biochem.* **150,** 76–85
41. Lorenz, H., Hailey, D. W., and Lippincott-Schwartz, J. (2006) *Nat. Methods* **3,** 205–210
42. Ruddy, D. A., Kronmal, G. S., Lee, V. K., Mintier, G. A., Quintana, L., Domingo, R., Jr., Meyer, N. C., Irrinki, A., McClelland, E. E., Fullan, A., Mapa, F. A., Moore, T., Thomas, W., Loeb, D. B., Harmon, C., Tsuchihashi, Z., Wolff, R. K., Schatzman, R. C., and Feder, J. N. (1997) *Genome Res.* **7,** 441–456
43. Meyer, M., Gaudieri, S., Rhodes, D. A., and Trowsdale, J. (2003) *Tissue Antigens* **61,** 63–71
44. Enroth, C., Eger, B. T., Okamoto, K., Nishino, T., Nishino, T., and Pai, E. F. (2000) *Proc. Natl. Acad. Sci. U.S.A.* **97,** 10723–10728
45. Lim, K., Ho, J. X., Keeling, K., Gilliland, G. L., Ji, X., Rüker, F., and Carter, D. C. (1994) *Protein Sci.* **3,** 2233–2244
46. Masters, S. L., Yao, S., Willson, T. A., Zhang, J. G., Palmer, K. R., Smith, B. J., Babon, J. J., Nicola, N. A., Norton, R. S., and Nicholson, S. E. (2006) *Nat. Struct. Mol. Biol.* **13,** 77–84
47. Henry, J., Mather, I. H., McDermott, M. F., and Pontarotti, P. (1998) *Mol. Biol. Evol.* **15,** 1696–1705
48. Laing, K. J., Purcell, M. K., Winton, J. R., and Hansen, J. D. (2008) *BMC Evol. Biol.* **8,** 42
49. Heid, H. W., Winter, S., Bruder, G., Keenan, T. W., and Jarasch, E. D. (1983) *Biochim. Biophys. Acta* **728,** 228–238
50. Mather, I. H. (1987) in *The Mammary Gland: Development, Regulation and Function* (Neville, M. C., and Daniel, C. W., eds) pp. 217–267, Plenum Publishing Corp., New York
51. McManaman, J. L., Russell, T. D., Schaack, J., Orlicky, D. J., and Robenek, H. (2007) *J Mammary Gland Biol. Neoplasia* **12,** 259–268
52. Buchheim, W. (1982) *Naturwissenschaften* **69,** 505–507
53. Wooding, F. B. P. (1977) *Symp. Zool. Soc. London* **41,** 1–41
54. McManaman, J. L., Palmer, C. A., Wright, R. M., and Neville, M. C. (2002) *J. Physiol.* **545,** 567–579
55. Adachi, T., Fukushima, T., Usami, Y., and Hirano, K. (1993) *Biochem. J.* **289**, 523–527
56. Keon, B. H., Ankrapp, D. P., and Keenan, T. W. (1994) *Biochim. Biophys. Acta* **1215,** 327–336
57. Pahl, H. L., and Baeuerle, P. A. (1994) *BioEssays* **16,** 497–502
58. Martin, H. M., Hancock, J. T., Salisbury, V., and Harrison, R. (2004) *Infect. Immun.* **72,** 4933–4939
59. Vorbach, C., Harrison, R., and Capecchi, M. R. (2003) *Trends Immunol.* **24,** 512–517
60. Admyre, C., Johansson, S. M., Qazi, K. R., Filén, J. J., Lahesmaa, R., Norman, M., Neve, E. P., Scheynius, A., and Gabrielsson, S. (2007) *J. Immunol.* **179,** 1969–1978